Metallocene Ethylene-*co*-5,7-Dimethylocta-1,6-Diene Copolymers Crosslinked by Electron Beam Irradiation: A Tunable Alternative

María L. Cerrada*, Rosario Benavente, Marta Fernández-García, Ernesto Pérez

Instituto de Ciencia y Tecnología de Polímeros (CSIC)

Juan de la Cierva 3, 28006 Madrid, SPAIN

and

João M. Campos, M. Rosário Ribeiro

Instituto de Ciência e Engenharia de Materiais e Superfícies – ICEMS, Instituto Superior Técnico - IST, Departamento de Engenharia Química e Biológica, Universidade Técnica de Lisboa– UTL, Av. Rovisco Pais, 1049-001 Lisboa, PORTUGAL

Abstract

Ethylene-*co*-5,7-dimethylocta-1,6-diene copolymers (CEDMO) with different molar DMO contents incorporate double bonds in the lateral chains that facilitate the development of crosslinkings in the resulting polymeric material after electron-beam (EB) irradiation. By effect of such irradiation, crystallization is delayed but crystallinity remains practically constant after melting and further cooling of irradiated specimens. Crystallinity, crystallite thickness and gel content are key parameters in the mechanical performance of these CEDMO copolymers. Consequently, the controlled incorporation of non-conjugated dienes into the polyethylene structure appears as an alternative strategy for tuning mechanical response in crosslinked polyolefins. Moreover, the resulting materials exhibit a good thermal stability.

Keywords:

Ethylene-co-5,7-dimethylocta-1,6-diene copolymers, electron-beam irradiation, crystallization, thermal stability, crystallites, storage modulus.

Corresponding authors: mlcerrada@ictp.csic.es (MLC)

Introduction

Polyethylene (PE) is one of the most important thermoplastics but its use in certain applications is restricted due to its low melting point, solubility or swelling in hydrocarbons and tendency to crack when stressed. In an effort to tackle these disadvantages there has been considerable work based on the crosslinking of PE. The discovery in the late 1950s that polyethylene properties could be enhanced by radiation crosslinking was a tremendous success at that time and it can be said that without it the development of the entire radiation processing industry would not be as robust as it is today.[1] Radiation crosslinked polyethylene is the basis for many jacketing compounds in wires and cables and for heat shrinkable films and tubing, which are the largest market segments using electron beam processing. Crosslinks between the polyethylene chains give rise to a better dimension stability during heat exposure because of the formation of a three dimensional network. This network not only improves the heat resistance but also makes the material more resistant towards chemicals and stress cracking, which makes it a very durable material.[2] In addition to this favorable effect on the PE mechanical behavior, electron beam irradiation leads as well to the sterilization of the polymer, this fact being very interesting for its applications in the fields of medical devices[3] and packaging industries.

Different procedures, in addition to the electron beam irradiation, are employed for the initiation of crosslinking in PE, all of them involving the formation of polyalkene macroradicals at some stage of the process. They include thermal decomposition of organic peroxides,[4-6] high energy irradiation using gamma rays,[7-9] and grafting of silane groups, which form crosslinks via hydrolysis of silanol moieties.[10] Some other protocols[2] are less frequently used or have only been investigated in the laboratory, and they comprise, among others: high-frequency heating, initiation by thermal decomposition of azo-esters or ethers, UV irradiation, redox initiation and free radical-initiated grafting of various moieties onto polyalkene chains. A recent investigation was focused on a different strategy based on the preparation of unsaturated polyolefins through the copolymerization of ethylene with non-conjugated dienes and their further EB irradiation.[11] This route takes advantage of the use of metallocene catalysts[12-15] leading to the synthesis of copolymers with narrow molecular weight distributions and with the side branches randomly distributed along the polymer backbone. The 5,7-dimethyl-1,6-octadiene (DMO) is chosen as comonomer since it has a vinylic double bond that can be polymerized with these metallocene catalysts whereas the presence of substituents on the second double bond inhibits its polymerization. In this way, pendant double bonds located within lateral branches are capable of being crosslinked in these ethylene-co-5,7-dimethylocta-1,6-octadiene (CEDMO) copolymers.

The morphology and, consequently, the properties of polyethylene change as a result of how crosslinking has occurred as well as other characteristics like molecular weight. A main difference exists between polyethylene (PE) crosslinked by thermal decomposition of peroxides

and by irradiation because in the former case, crystallization proceeds from a crosslinked melt, while in the latter crosslinking takes place in the solid state. Therefore, the degree of crystallinity in peroxide-crosslinked samples decreases and is more or less constant after repeated melt-crystallization cycles, unlike in irradiation crosslinked PE where no change is observed after irradiation-induced crosslinking. However, a decrease in the crystallized portion is proved after the first melt-crystallization cycle in these irradiation-induced crosslinked PEs similar to the one found in peroxide-initiated crosslinking.[2]

The article previously reported on irradiated CEDMO copolymers[11] was primarily focused on an evaluation of different crystalline features shown by the distinct as-processed irradiated copolymers depending on composition and doses. Then, knowledge on crystal lattice constants (from X ray measurements at wide angle region, WAXS) and on crystallite size (from X ray profiles at the small angle region, SAXS) were obtained using real-time variable-temperature experiments employing synchrotron radiation. In addition, preliminary mechanical information was achieved from microhardness measurements. Once learnt on the formation of crosslinkings and on the structural characteristics exhibited by the "as-processed" irradiated specimens, the thermal and viscoelastic characterization of those samples is addressed in this article as well as the analysis of how crystallinity and long spacing features change after the first melting process, i.e., during the further crystallization and subsequent melting processes. To attain these goals several techniques have been required: differential scanning calorimetry, DSC, for the evaluation of the melting and crystallization transitions, real-time variable temperature SAXS experiments for knowledge on long spacing values; thermogravimetric analysis for thermal stability, dynamic thermal analysis for examining the mechanical response, which has been compared with the results obtained from microhardness measurements.

Experimental Part

Copolymerizations of ethylene and 5,7-dimethylocta-1,6-diene were performed as described elsewhere[11,16] and several ethylene-*co*-5,7-dimethylocta-1,6-diene copolymers, with different comonomer content, were obtained. They were labeled as CEDMO followed by two numbers that indicate their molar composition in DMO. The HDPE homopolymer analyzed was similarly named as CEDMO0.0.

Preparation of specimens

The different CEDMO copolymers and the corresponding homopolymer analyzed in the current paper were obtained as films by compression molding in a Collin press between hot

plates (150 °C) at a pressure of 1.5 MPa for 5 min for their thermal and structural characterization as well as the analysis of their mechanical response. Thickness ranged from 500 to 550 μm. Each one of the samples was processed by a fast quench between plates cooled with water after its melting in the press.

Irradiation of specimens

Electron beam (EB) irradiation was carried out at IONMED (an industrial installation) in atmospheric air at ambient temperature using a 10 MeV Rhodotron accelerator. All polymeric films were irradiated on one side using a current of 5 mA such that the polymeric samples were exposed to an irradiation dose of about 33.3 kGy per pass. Several passes under these conditions were required for high irradiation doses. The EB irradiation doses are ranged throughout this work from 33 to 233 kGy. A label related to identification of the dose applied is added to the name of each copolymer. Therefore, NR represents non-irradiated samples and A, B, C and D upper cases indicate the dose: 33, 67, 133 and 233 kGy, respectively.

Gel content determination

The gel content (insoluble fraction) of the different specimens was determined gravimetrically, according to ASTM D 2765, using a 16-h Soxhlet extraction cycle, with p-xylene as the solvent at 140°C. The polymeric samples were cut into small pieces and placed in a pre-weighed stainless steel, fine wire mesh. After the extraction cycle, the samples were washed with acetone and vacuum-dried to a constant weight. The gel content was calculated as the percentage ratio of the final weight of the insoluble polymeric fraction to its initial weight previous extraction.

X-Ray scattering measurements

The X-ray synchrotron study was performed in the soft-condensed matter beamline A2 at Hasylab (Hamburg, Germany), working at a wavelength of 0.150 nm. The experimental setup includes a specimen holder, a MARCCD detector for acquiring two-dimensional SAXS patterns (sample-to-detector distance being 260 cm) and a linear detector for 1D WAXS measurements (distance 21 cm). A sample of crystalline PET was used for WAXS calibration and the different orders of the long spacing of rat-tail cornea (L = 65 nm) were utilized for the SAXS detector. The two-dimensional X-ray patterns from the MARCCD detector were processed with the FIT2D program of Dr. Hammersley (ESRF) and converted into one-dimensional arrays after normalization for the intensity of the primary beam and subtraction of the scattering of an empty sample.

Differential Scanning Calorimetry

Calorimetric analyses were carried out in a Perkin-Elmer DSC7 calorimeter, connected to a cooling system and calibrated with different standards. The sample weights ranged from 6 to 7.5 mg. A temperature interval from -50 °C to 150 °C was studied and the used heating rate was 10 °C·min^{-1}. For crystallinity determinations, a value of 290 J·g^{-1} was taken as the enthalpy of fusion of a perfectly crystalline material.[17,18]

Thermogravimetric analysis

The weight loss was estimated by thermogravimetry using the TA Instruments TGA Q500 equipment working under an inert atmosphere. The equipment was calibrated according to standard protocols. The sample weights ranged from 4 to 6 mg, and the heating rate was 10 °C·min^{-1}.

Dynamic-mechanical properties

Dynamic mechanical relaxations were measured with a Polymer Laboratories MK II Dynamics Mechanical Thermal Analyzer, working in a tensile mode. The storage modulus, E', loss modulus, E'', and the loss tangent, tan δ, of each sample were obtained as function of temperature over the range from –150 to 150 °C (this last temperature was modified depending on the melting temperature of the sample), at fixed frequencies of 1, 3, 10, 30 Hz, and at a heating rate of 1.5 °C·min^{-1}. Strips around 2.2 mm wide and 15 mm length were cut from the molded sheets. The apparent activation energy values were calculated on the basis of tan δ according to an Arrhenius-type equation, considering an accuracy of ±1 °C in the temperature assignment from the maxima.

Microhardness Determination

A Vickers indentor attached to a Leitz microhardness tester was used to perform microindentation measurements, undertaken at 23 °C. A contact load of 0.98 N and a contact time of 25 s were employed. Microhardness, MH, values (in MPa) were calculated according to the relationship:[19]

$$MH = 2 \sin 68° \, P / d^{2} \qquad [1]$$

where P (in N) is the contact load and d (in mm) is the diagonal length of the projected indentation area. Diagonals were measured in the reflected light mode within 30 s of load removal, using a digital eyepiece equipped with a Leitz computer-counter-printer (RZA-DO).

Results and discussion

The gel content estimated in the irradiated samples is strongly dependent on DMO composition and irradiation dose, as depicted in Figure 1 and previously reported.[11] This gel is related to the network structure developed in the amorphous regions, which is insoluble in the solvent, whereas the sol content corresponds with the linear portion of the polymer in both amorphous and crystalline regions. It should be expected that the non-irradiated specimens would exhibit a gel content equal to zero. However, as seen in Figure 1, the non-irradiated CEDMO1.9 copolymer (CEDMO1.9-NR specimen) shows an important gel content. This initial crosslinking is mainly generated during the initial processing as films at 150 °C.[11]

The dependence on composition of crosslinking level for the homopolymer and the other two copolymers is clearly seen. Thus, it gradually increases at the smaller doses up to reach a maximum value of around 80% in the CEDMO0.0 homopolymer while incorporation of DMO comonomer, even in a molar fraction as low as 0.7, provokes a significant raise of gel content at the smallest doses. Around five times in CEDMO0.7-A compared with CEDMO0.0-A and about the double in CEDMO0.7-B respect to CEDMO0.0-B. The maximum value attained is also higher: 90% *vs* 80% in the CEDMO0.0-D homopolymer. A slightly higher DMO addition leads to the almost complete crosslinking content at 67 kGy, the value at 33 kGy being around 90%.

Figure 2 shows the DSC traces for the different non-irradiated and irradiated samples and the semicrystalline character of all these samples is clearly deduced. They crystallize in the regular orthorhombic lattice characteristic for polyethylenes and copolymers,[20,21] displaying the (110) and (200) diffraction peaks in their WAXS profiles.[11,15] Looking first at the NR specimens represented in Figure 2, an important depression of the melting temperature (T_m) is observed as DMO is incorporated and the content in copolymer increases. This feature is ascribed to the diminishment of the respective crystallite sizes observed in Figure 3. These most probable crystal sizes represented, l_c, are obtained from the WAXS and SAXS results at room temperature in the “as-processed” non-irradiated and irradiated samples.[11] Moreover, the melting enthalpy is also significantly reduced with incorporation of DMO in the copolymers and, consequently, the crystallinity reached is considerably lowered (see results in listed in Table 1). However, the crystallinity reduction is not strongly dependent on DMO composition in the range explored in these CEDMO copolymers[15] lower than 2 mol% in these pendant unsaturated groups. The counits copolymerized here with ethylene are rather bulky and the capability of being incorporated to the PE crystalline lattice does not practically exist. Therefore, their high volume triggers a high hindrance for the PE crystallization, which is almost similar at this composition range as reported in Table 1. The interruption of this PE chain regularity just mentioned can be also seen from a slight broadening of the melting region (see Figure 2), this

fact being associated with the wider crystal size distributions found in the copolymers with different DMO contents.

Concerning the effect of irradiation process, DSC crystallinity estimated from the first heating process remains practically unchanged at a given copolymer independently of the dose used, as seen from the f_c^{m1} results reported in Table 1. However, the melting temperature along this initial melting process, T_{m1}, undergoes a slight diminishment with irradiation dose related to a reduction in the crystallite size assessed at room temperature (see Figure 3).

Crosslinking takes place in solid state in these copolymers under study. The crystalline parameters found during the first heating process at a given irradiated specimen remain rather constant (crystallinity values) or undergo a slight reduction (most probable crystal sizes and melting temperatures) when compared to its non-irradiated homologous one. Then, the mechanical performance in these irradiated specimens is not expected to be worsened, as will be discussed afterward, due to the almost constancy in these crystalline characteristics and to their great importance on the final response.

As proved up to now, the main structural changes caused by irradiation have occurred in the amorphous region (see Figure 1), probably via hydrogen abstraction from the saturated polymer backbone and recombination of the free radicals along the polymer chain. Then, an important aspect should be addressed following this first melting process. How do the crosslinked macrochains initially located in the amorphous regions modify the further crystallization capability of these copolymers? It is well-known that if the formation of crosslinking occurs in the molten state through the incorporation of peroxides or functional monomers, a significant decrease of the degree of crystallinity is observed when crystallization proceeds during the subsequent processing.[2,4,5] However, what does it happen in these non-conjugated diene CEDMO copolymers? To answer this question, the crystallization analysis and the additional study of how the second heating run occurs are performed by DSC and complemented by SAXS synchrotron study.

Figure 4 shows DSC crystallization curves for all the samples at the different doses. A very slight shift of crystallization temperature is observed with irradiation dose in the CEDMO0.0 homopolymer. However, copolymers present a more significant displacement of T_c to lower temperatures (around 6 °C in the dose interval analyzed). The presence of crosslinked chains modifies at some extent the rate of crystallization, delaying the formation of crystallites and leading probably to smaller crystals. However, there is not a significant DSC crystallinity reduction in these copolymers, this being more important in the CEDMO0.0 homopolymer.

The subsequent DSC heating run points out that melting temperatures are slightly lowered, around 3 °C for the highest dose, compared to those found during the first melting

process in the different specimens (see results in Table 1). This feature seems to support the assumption of the presence of smaller crystallites. To corroborate this hypothesis, crystallization and second melting processes are followed in some specimens by real-time variable temperature SAXS experiments. Some features can be clearly deduced from the profiles represented in Figure 5 that correspond to the CEDMO0.0 and CEDMO1.9 samples non-irradiated and irradiated at the highest dose. Concerning the CEDMO0.0 homopolymer, it is observed that crystallization is slightly delayed, location of the SAXS peak is moved to higher 1/d values and its broadness is enlarged as effect of irradiation. In the copolymer, the decrease in rate of crystallization is also clear as well as the shift of crystallization to lower temperature because of the irradiation.

More discerning information can be achieved from the plots of normalized area variation and long spacing values with temperature depicted in Figures 6 and 7. Regarding the CEDMO0.0 homopolymer, if crystallization and subsequent melting processes are compared between the non-irradiated and irradiated at the highest dose specimens, a slight shift of crystallization temperature, T_c, is seen while an important decrease of T_m is detected (see plots A and C of Figure 6), corroborating the facts observed by DSC. Moreover, the long spacing values obtained after crystallization are considerably smaller in the irradiated CEMO0.0-D sample than in the CEDMO0.0-NR one (see Figure 7) as well as its degree of DSC crystallinity (Table 1). All of these features support the assumption that crystallization is delayed and crystallite size diminishes with irradiation dose and those smaller crystals melt at lower T_m temperature. Additionally, a secondary crystallization process is clearly observed. Consequently, a two-step long spacing variation is observed in the temperature interval from 100 to 60 °C.

On the other hand, it is noticed that long spacing values are crystallization rate dependent in the CEDMO0.0-NR sample and rather independent when irradiation is applied. A cooling rate of 12 °C/min allows developing more perfect crystallites than a quenching process and, accordingly, long spacing values of initial melting process of CEDMO0.0-NR are inferior to those found in the CEDMO0.0-NR second melting. The influence of crystallization rate is less important in the irradiated CEDMO0.0-D sample.

In relation to the CEDMO1.9 copolymer, it has to be said that a considerable displacement of T_c is observed when comparing CEDMO1.9-NR and CEDMO1.9-D samples. However, the T_m of the following melting process remains practically unchanged (see plots B and D in Figure 6). The changes in degree of crystallinity with irradiation dose determined from DSC curves point out to a less significant variation than that found in CEDMO0.0 specimens. A relative similarity of long spacing values for the CEDMO1.9-NR and CEDMO1.9-D samples is also observed (Figure 7), *i.e.*, rather small variation of crystallite size is noticed in this copolymer and, consequently, T_m does not considerably decrease with irradiation dose.

Figure 8A represents the thermogravimetric curves found in all of the different non-irradiated specimens and some of those irradiated ones (B and D doses). The temperature of maximum degradation (see Figure 8B) is not very dependent on DMO comonomer composition, although degradation starts to take place at considerably lower temperatures as DMO content increases, mainly for the highest composition. The presence of oxidized species in CEDMO1.9-NR reduces 11 °C the maximum degradation temperature, T^{max}, with respect to the value obtained in the CEDMO0.0-NR. However, a variation of only 3 °C is found in the irradiated samples at the highest dose (see Table 1). Although thermal stability decreases with DMO content, this worsening is rather acceptable in this composition interval of interest (it should be reminded that higher DMO contents would lead to a much important undesirable crystallinity reduction). The loss weight plot of irradiated D samples shows that CEDMO1.9-D specimen keeps around the 40% of its initial weight. The chemical structures developed during the decomposition process are probably of cyclic nature and, then, do not completely decompose under the inert atmosphere used in this investigation.

Figure 9A shows the variation of the storage modulus (E′) and loss tangent (tan δ) for the different specimens. In the upper plot, it is observed that the storage modulus significantly decreases as DMO content is incorporated, and this reduction is mainly noticeable at temperature above 0 °C. Differences are ascribed to changes in crystallinity and, then, the distinct CEDMO copolymers exhibit analogous values in the temperature range examined since they show similar degree of crystallinity. However, these values are considerably lower than those derived from CEDMO0.0 homopolymer. The effect of irradiation on the storage modulus is not straightforward, as seen in Figure 10, where the E′ values at room temperature are represented for all of the specimens. This fact was also observed from microhardness (MH) measurements at the same temperature, as previously described[11].

Three different parameters play a key role in the mechanical response of these specimens. These are: crystallinity, crystallite thickness and the crosslinking degree within the amorphous regions. For instance, a decrease of E′ is seen in the irradiated specimens at A and B doses in the CEDMO0.0 homopolymer. The increase in crosslinking content within amorphous chains seems not to be enough to compensate reduction in crystallite size although crystallinity remains practically constant. However, MH increases in the irradiated specimens, fact that seems to indicate that at the surface the effect of crosslinkings is rather important[11]. For the copolymers, the balance between decreasing crystallite thickness and increasing crosslinking density is again the key player for E′ or MH values to be enlarged or reduced. What is important is that irradiation does not worsen the mechanical performance of these irradiated copolymers. In addition, it is expected that their mechanical response would be similar after recycling

processes since the crosslinking density remains constant and crystallinity degree (see Table 1) as well as crystallite thickness do not vary much (see Figure 7).

In relation to relaxation processes, the loss tan δ plots represented in Figure 9B show the existence of two clear main processes whose intensity and location is slightly dependent on DMO content, labeled as γ and α in order of increasing temperatures. Moreover, an additional relaxation is observed. It is named as β and is located between the γ and α processes. This relaxation is also reported in low density, LDPE, linear low density, LLDPE, and ethylene copolymers.[22-26] The β mechanism appears in the CEDMO0.7 and CEDMO1.0 copolymers as a shoulder of the α relaxation while in the CEDMO1.9 its intensity significantly increases and the overlapping with the α process is deeper because of the shift of this last one to lower temperature.

The γ relaxation in PE was firstly attributed to crankshaft movements of polymethylenic chains[27] but there remains no clear consensus regarding the details of the underlying motional process.[28,29] This γ process is also found in polyesters containing oxyethylene spacers, where the oxygen atom plays an equivalent role than the methylenic groups.[30-32] This type of motion requires chains containing sequences of three or more methylenic units and takes place in the amorphous regions. Figure 9B displays that the location and intensity of γ peak does not practically modify with incorporation of the two lowest DMO contents. The crystallite thicknesses are lowered in CEDMO1.9 respect to the other copolymers and, then, mobility constraints become reduced and relaxation occurs at slightly lower temperatures. The incorporation of higher DMO content disrupts the consecutive methylenic units and, accordingly, intensity diminishes.

The relaxation that appears at the highest temperature, α relaxation, is associated with vibrational and reorientational motions within the crystallites.[33,34] The melting of the crystallites is overlapped with this process at high temperatures. As discussed for the motions within the amorphous regions, those occurring in the crystals become easier as DMO content increases because of the reduction in crystallinity and crystallite size. Consequently, the location of the α relaxation is shifted to lower temperatures (see Figure 9B). The irradiation effect primarily affects the crystallite size (see Figure 3) of a given copolymer and, therefore, motions in crystalline regions can take place at lower temperatures, slightly shifting the location of the viscoelastic mechanism.

Conclusions

The existence of double bonds in the lateral chains incorporated by copolymerization of ethylene with DMO significantly facilitates the development of crosslinkings after application of irradiation doses. The different polymeric materials synthesized are semicrystalline and the crystalline characteristics (T_m, T_c, crystallinity, crystallite size) are strongly dependent on composition, mainly from CEDMO0.0 to CEDMO0.7. As result of irradiation, a higher lamellar thickness reduction is observed as DMO content is lowered: the variation of crystallite thickness is around 8% for the CEDMO0.7 series and about 4% or 2% for the CEDMO1.0 or CEDMO1.9 specimens, respectively. Moreover, presence of the crosslinked chains modifies at some extent the rate of crystallization, delaying the formation of crystallites in the irradiated specimens.

In the homopolymer, the long spacing values obtained after crystallization are in the irradiated CEMO0.0-D sample considerably smaller than in the CEDMO0.0-NR one as well as its degree of DSC crystallinity and, then, T_m significantly shifts to lower temperatures. In relation to the different copolymers, a more important displacement of T_c is observed when the non-irradiated and irradiated samples are compared at a given CEDMO copolymer. However, the T_m values of the subsequent melting process vary much less than those found in the homopolymer, and changes of degree of crystallinity are rather small in comparison. A relative similarity of long spacing values for the CEDMO1.9-NR and CEDMO1.9-D samples is also seen, proving a rather small variation of crystallite size with irradiation dose.

The presence of oxidized species in CEDMO1.9-NR reduces 11 °C the maximum degradation temperature, T^{max}, with respect to the value obtained in the CEDMO0.0-NR. However, a variation of only 3 °C is found in the corresponding irradiated samples at the highest dose (see Table 1). This loss of thermal stability is rather acceptable in this interval of compositions. In addition, it seems that these materials might be recycled keeping their overall structural, thermal and mechanical behavior.

Finally, all the CEDMO copolymers show three viscoelastic mechanisms. Crystallinity, crystallite thickness and crosslinking degree play a key role in the mechanical performance observed: stiffness and location of distinct relaxations. Incorporation of controlled DMO composition on polyethylene seems to be an appropriate and tunable technology for tailoring structural characteristics and, accordingly, the mechanical response. These features might offer new possibilities in the large market of radiation crosslinked polyethylenic products.

Acknowledgements:

The authors are grateful for the financial support of Ministerio de Ciencia e Innovación (project MAT2007 65519-C02-01), Exchange Collaboration Program CSIC/FCT (projects 2005PT0033 / Proc. 4-1-1 Espanha 2006/2007 and 2009PT0026 / Proc. 441.00 CSIC), and Fundação para a Ciência e a Tecnologia, Programa Operacional Ciência Tecnologia e Inovação (POCTI) do Quadro Comunitário de Apoio III e comparticipado pelo Fundo Comunitário Europeu FEDER (Project PDCT/CTM/66408/2006). The synchrotron work, performed at DESY, leading to these results has received funding from the European Community's Seventh Framework Programme (FP7/2007-2013) under grant agreement n° 226716. We thank the collaboration of the Hasylab personnel in the soft-condensed matter beamline A2, especially Dr. S. S. Funari.

Table 1. Melting and crystallization temperatures determined by DSC (T_{m1} and T_{m2}, estimated from the first and second heating run respectively, and T_c), degree of crystallinity found during first heating, cooling and second heating runs (f_c^{m1}, f_c^{C} and f_c^{m2}, respectively) and temperature of maximum degradation (T^{max}) obtained from thermogravimetric analysis, for the different samples and irradiation doses.

specimen	T_{m1} (°C)	f_c^{m1}	T_c (°C)	f_c^{C}	T_{m2} (°C)	f_c^{m2}	T^{max} (°C)
CEDMO0.0-NR	133	0.63	112	0.67	134	0.67	491
CEDMO0.0-A	132	0.64	112	0.64	132	0.66	489
CEDMO0.0-B	132	0.63	112	0.64	131	0.65	489
CEDMO0.0-C	131	0.64	112	0.60	129	0.62	484
CEDMO0.0-D	131	0.64	111	0.59	127	0.62	484
CEDMO0.7-NR	114	0.42	102	0.43	113	0.43	486
CEDMO0.7-A	114	0.42	99	0.40	111	0.43	486
CEDMO0.7-B	113	0.43	97	0.40	110	0.43	485
CEDMO0.7-C	113	0.42	96	0.41	110	0.41	485
CEDMO0.7-D	113	0.43	96	0.41	110	0.41	484
CEDMO1.0-NR	111	0.37	100	0.40	111	0.40	484
CEDMO1.0-A	110	0.38	97	0.38	108	0.40	484
CEDMO1.0-B	110	0.37	96	0.36	107	0.38	482
CEDMO1.0-C	110	0.37	95	0.38	107	0.38	484
CEDMO1.0-D	110	0.38	93	0.38	107	0.38	484
CEDMO1.9-NR	105	0.40	91	0.40	104	0.41	480
CEDMO1.9-A	104	0.42	89	0.40	103	0.41	480
CEDMO1.9-B	104	0.42	87	0.40	102	0.41	480
CEDMO1.9-C	104	0.39	85	0.40	102	0.40	481
CEDMO1.9-D	104	0.39	85	0.40	101	0.40	481

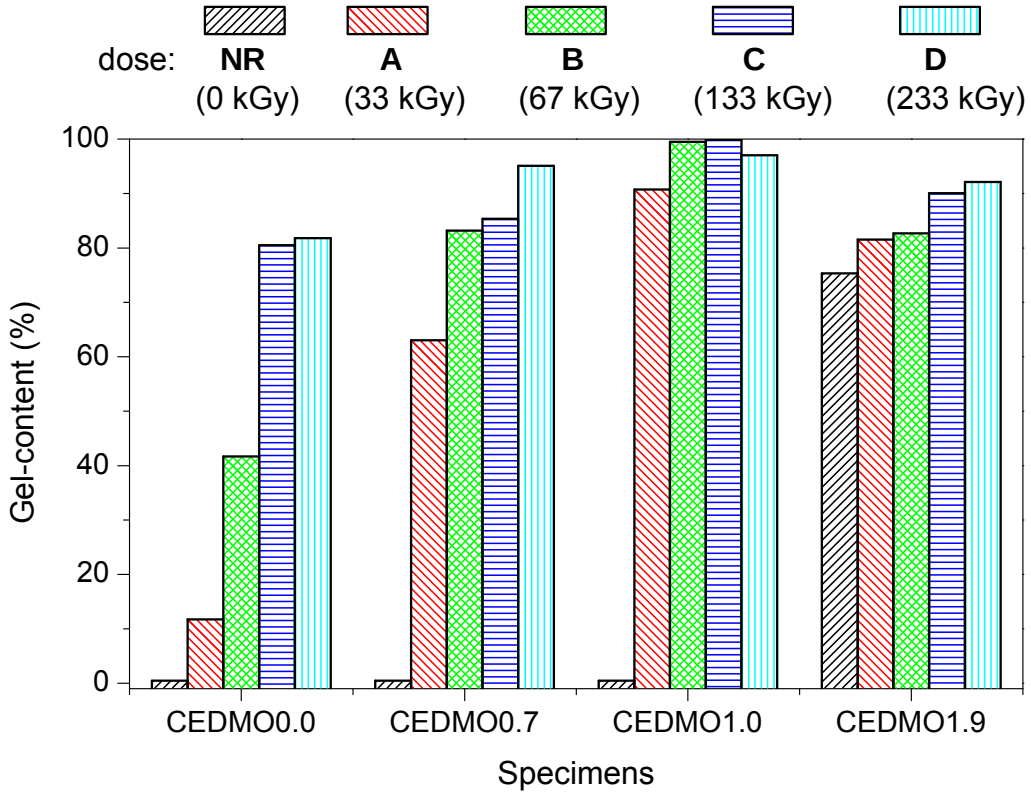

Figure 1. Effect of irradiation dose on gel content for the polyethylene homopolymer, CEDMO0.0, and its copolymers with different DMO contents.

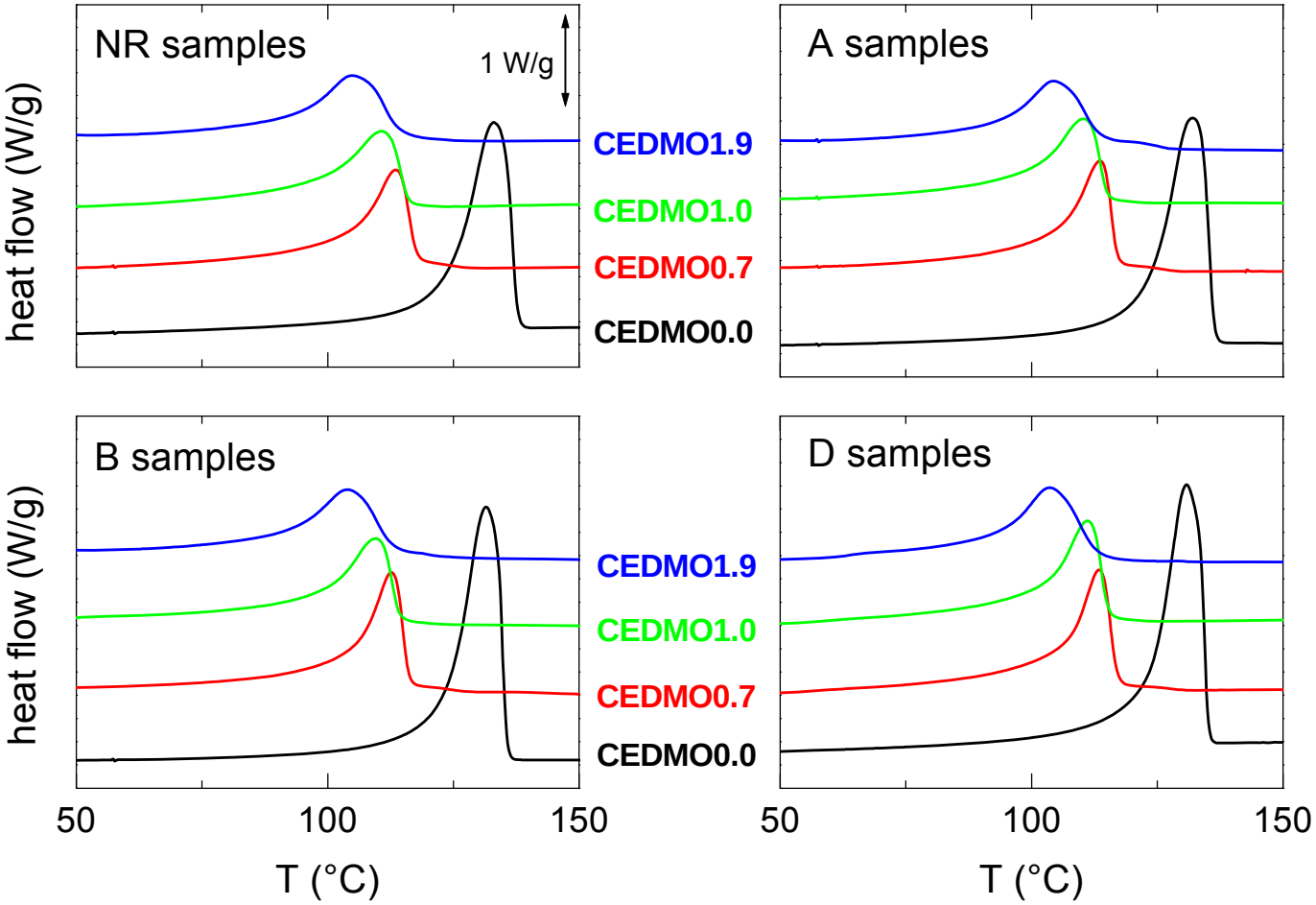

Figure 2. DSC melting curves for the homopolymer CEDMO0.0 and the different copolymer specimens non-irradiated and irradiated at different doses.

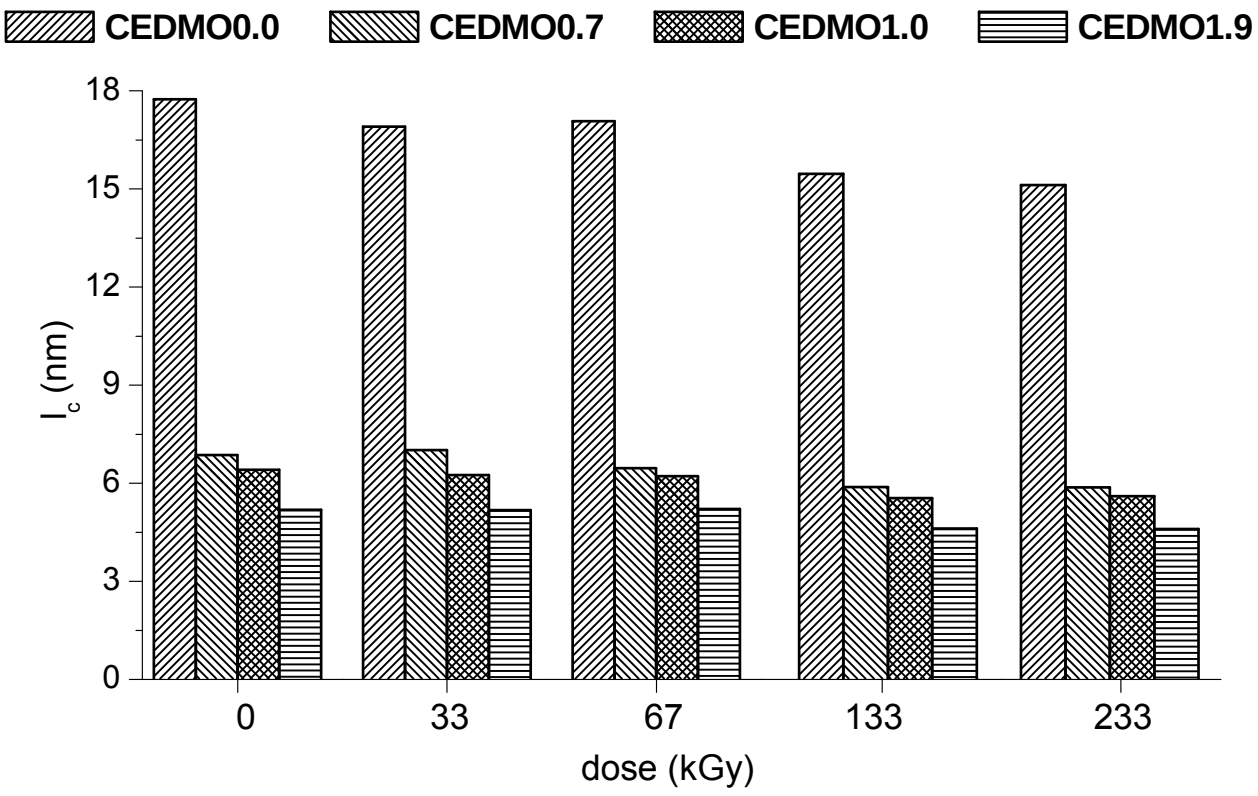

Figure 3. Most probable crystallite size at room temperature, determined from SAXS and WAXS profiles, for the different samples and irradiation doses.

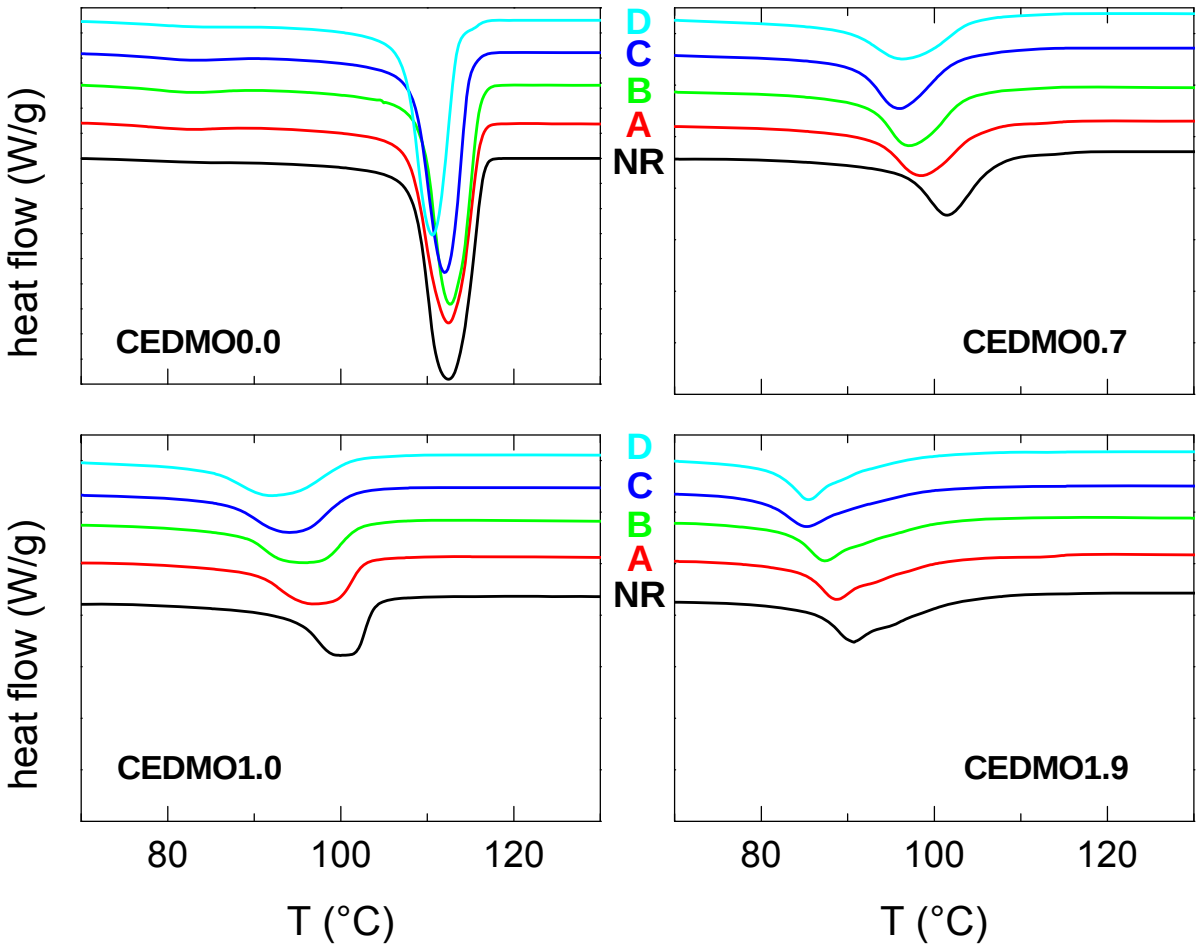

Figure 4. DSC crystallization curves for the homopolymer CEDMO0.0 and the different copolymer specimens non-irradiated and irradiated at the different doses.

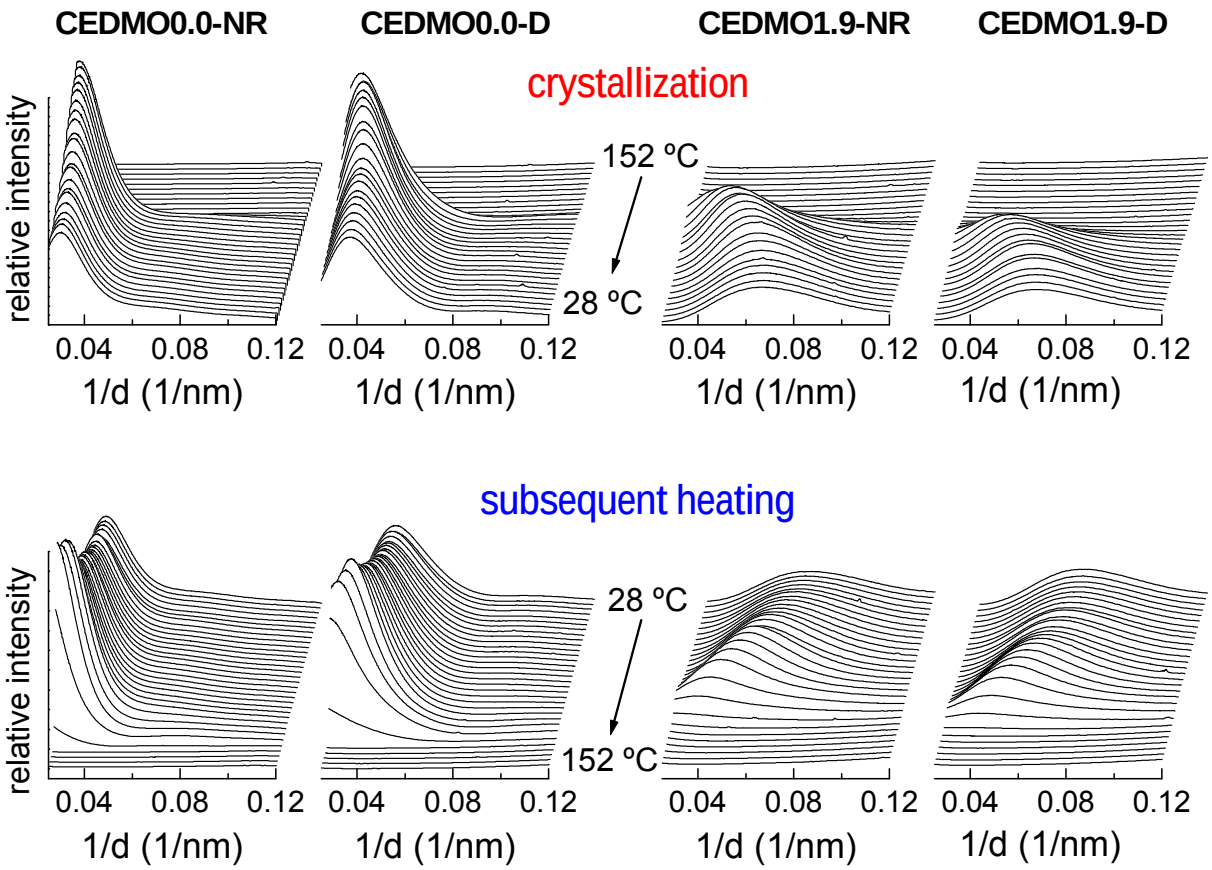

Figure 5. Real-time SAXS profiles, obtained with synchrotron radiation, in the non-irradiated and irradiated at 133 kGy specimens for the CEDMO0.0 homopolymer and CEDMO1.9. Profiles obtained during crystallization (upper plots) and the subsequent heating run (lower plots). The scanning rate for all of the specimens is 12 °C·min^{-1}.

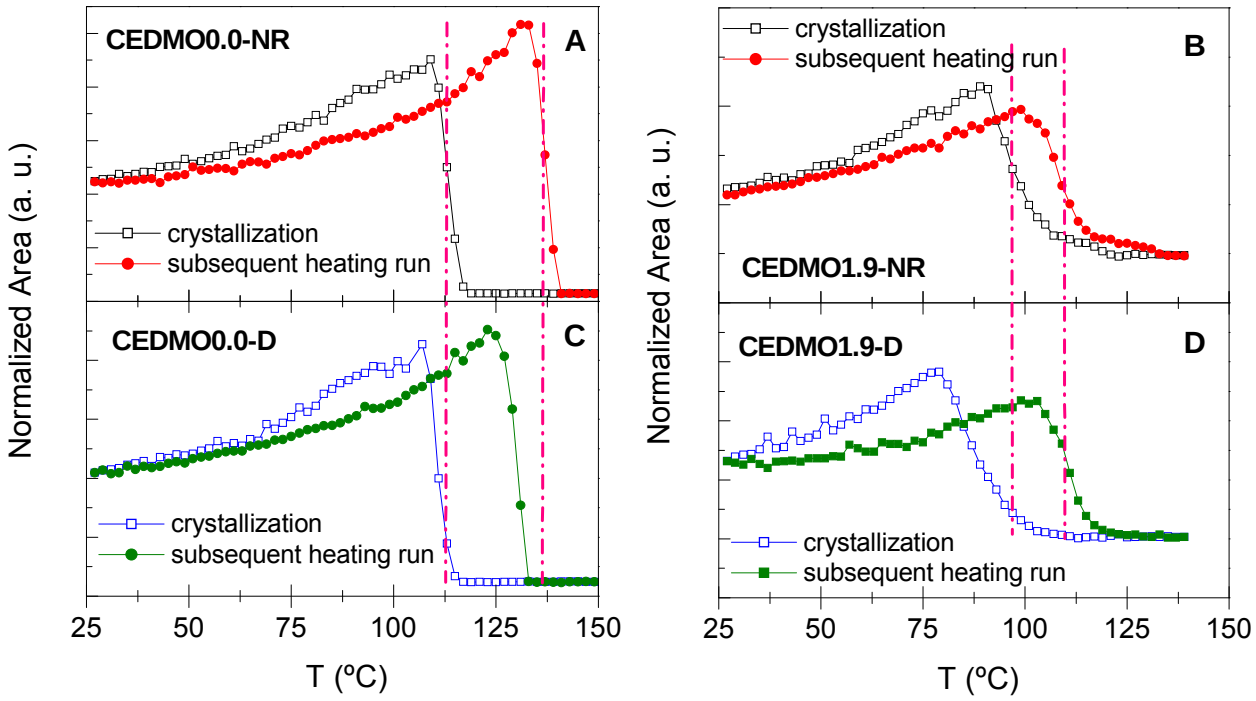

Figure 6. Temperature dependence of relative SAXS invariant of the specimens: A) CEDMO0.0-NR; B) CEDMO1.9-NR; C) CEDMO0.0-D and D) CEDMO1.9-D.

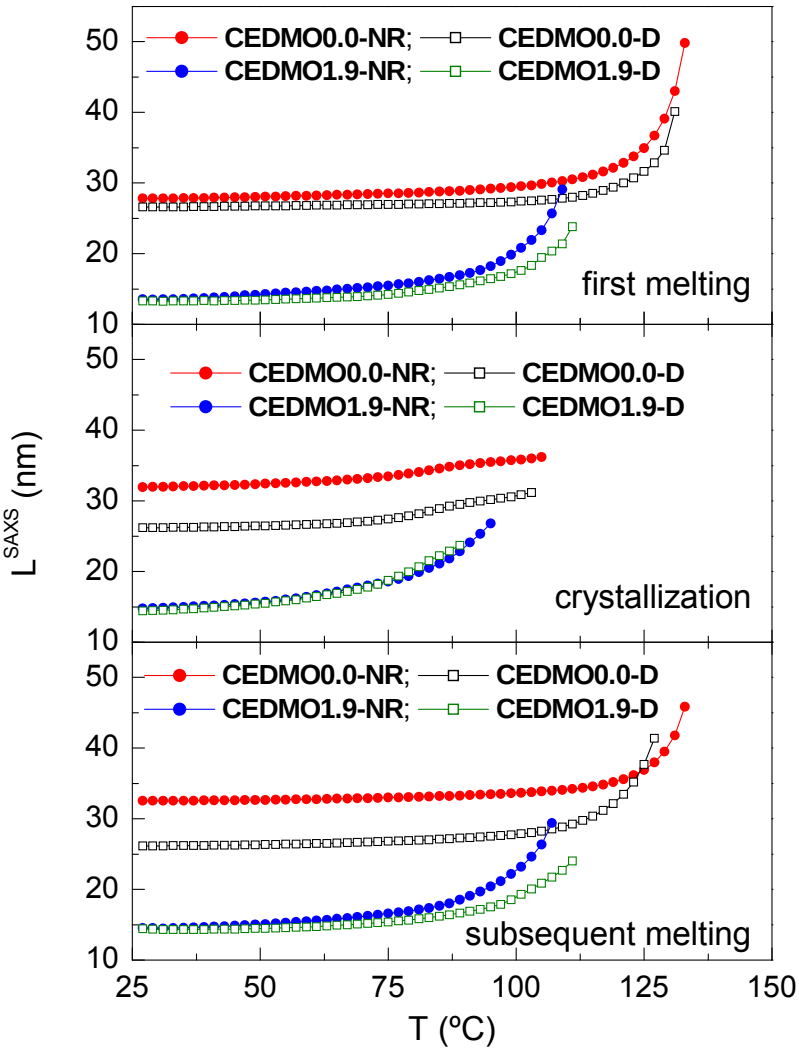

Figure 7. Effect of temperature on the long spacing for samples CEDMO0.0-NR, CEDMO0.0-D, CEDMO1.9-NR and CEDMO1.9-D during the first melting (top), crystallization from the melt (middle) and subsequent melting (bottom).

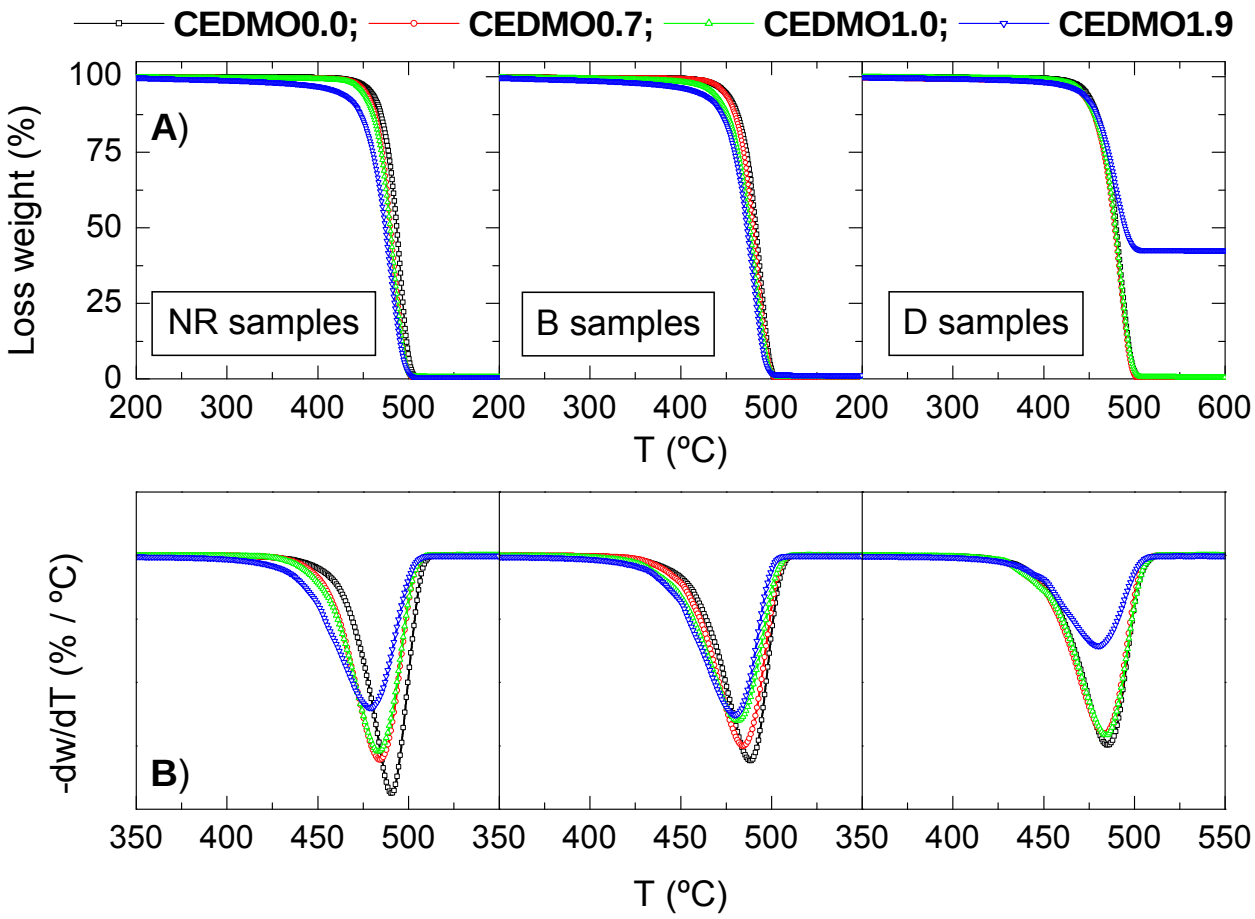

Figure 8. A) TG and B) DTG curves for the non-irradiated specimens and those irradiated at a dose of 67 kGy (B samples) and 233 kGy (D samples).

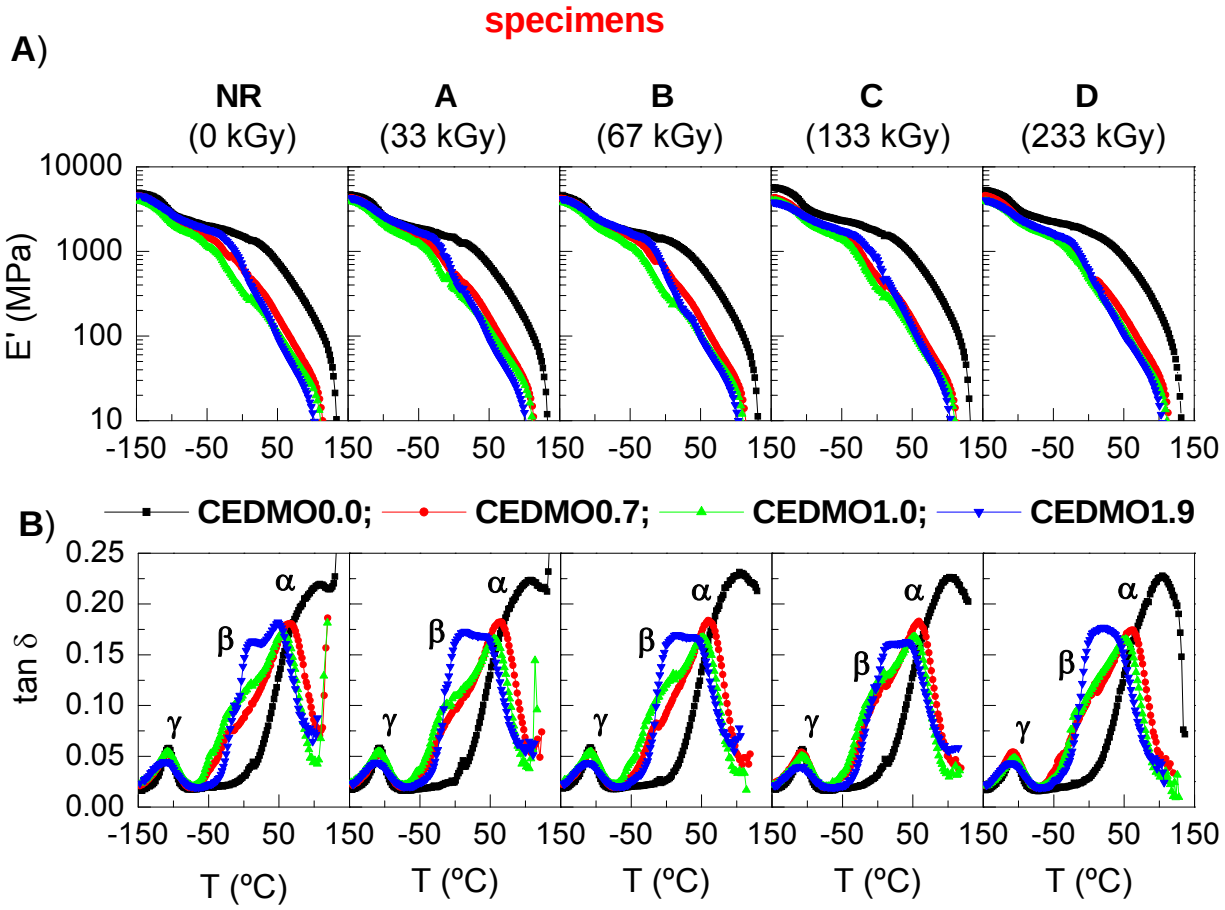

Figure 9. A) Variation of the storage modulus (E′) and B) dependence of tan δ on temperature, at 3 Hz, for all of the non-irradiated and irradiated CEDMO specimens.

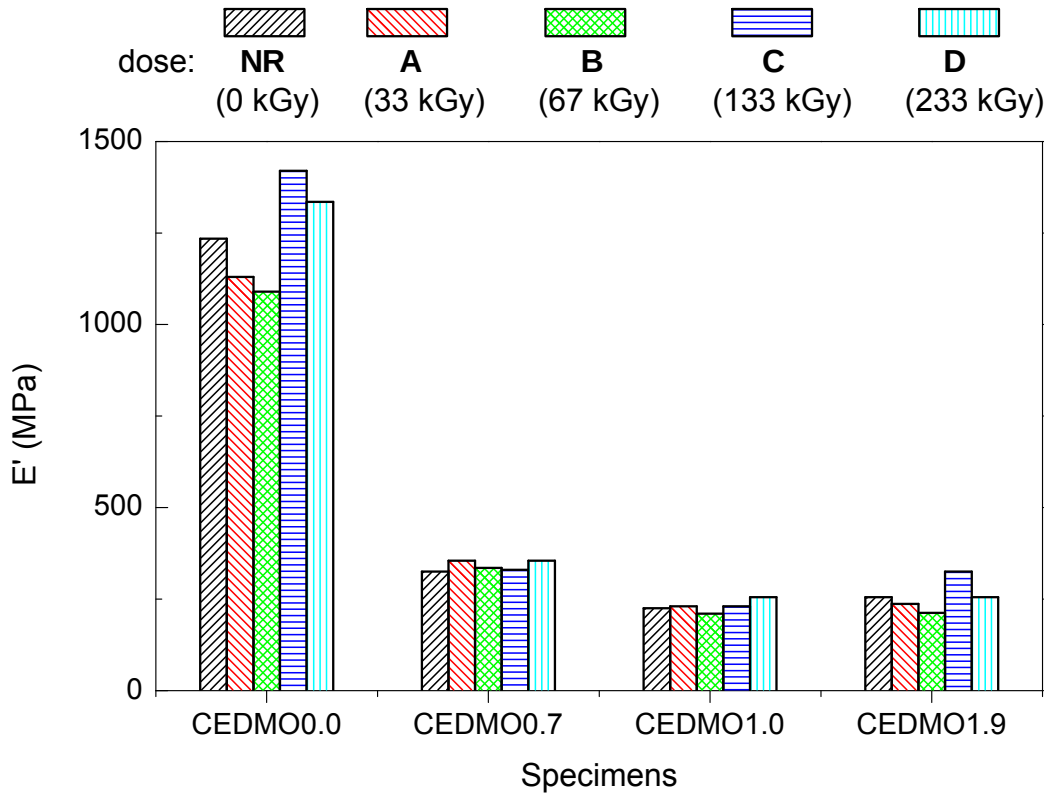

Figure 10. Elastic modulus values (E′) at room temperature as function of irradiation doses for the different polymeric materials analyzed: CEDMO0.0, CEDMO0.7, CEDMO1.0 and CEDMO1.9 from left to right.

References

[1] Charlesby A, Atomic Radiation and Polymers, Pergamon Press Ltd., New York, 1960, p. 198.

[2] Chodak I. Properties of cross-linked polyolefin-based materials. Prog Polym Sci 1995;20:1165-1199.

[3] Ratner BD, Hoffman AS, Schoen FJ, Lemons JE. In Biomaterials Science: An Introduction to Materials in Medicine. Academic Press, San Diego, CA, USA, 1996.

[4] Khonakdar HA, Morshedian J, Wagenknecht U, Jafari SH. An investigation of chemical crosslinking effect on properties of high-density polyethylene. Polymer 2003;44:4301-4309.

[5] Khonakdar HA, Jafari SH, Taheri M, Wagenknecht U, Jehnichen D, Haüssler L. Thermal and wide angle X-ray analysis of chemically and radiation-crosslinked low and high density polyethylenes. J App Polym Sci 2006;100:3264-3271.

[6] Andersson LHU, Hjertberg T. The effect of different structure parameters on the crosslinking behaviour and network performance of LDPE. Polymer 2006;47:200-210.

[7] Zhang L, Zhou M, Chen KG. Effects of structure multiplicity on mechanism of radiation cross-linking of polymers. Radiat. Phys. Chem. 1994;44:303-308.

[8] Abou Zeid HM, Ali ZI, Maksoud TMA, Khafagy RM. Structure-property behavior of polyethylene exposed to different types of radiation. J Appl Polym Sci 2000;75:179-200.

[9] Torrisi L, Visco AM, Campo N. Dose and dose-rate dependence of polyethylene irradiation with electron beams "in air". J Mater Eng Perform 2007;16:97-101.

[10] Wong WK, Varrall DC. Role of molecular-structure on the silane cross-linking of polyethylene - the importance of resin molecular-structure change during silane grafting. Polymer 1994;25:5447-5452.

[11] Cerrada ML, Benavente R, Fernández-García M, Pérez E, Campos JM, Ribeiro MR. Cross-linking in Metallocene Ethylene-co-5,7-Dimethylocta-1,6-Diene Copolymers initiated by Electron-Beam Irradiation. Polymer 2009;50:1095-1102.

[12] Pietikäinen P, Starck P, Seppälä JV. Characterization of comonomer distributions in ethylene diene copolymers by C-13-NMR, and using the segregation fractionation technique by DSC and DMTA. J Polym Sci, Part A: Polym Chem 1999;37:2379-2389.

[13] Santos JM, Ribeiro MR, Portela MF, Cramail H, Deffieux A. Transition metal complexes as catalysts for the homo- and copolymerisation of olefins and non-conjugated dienes. Macromol Chem Phys 2001;202:3043-3048.

[14] Santos JM, Ribeiro MR, Portela MF, Cramail H, Deffieux A, Antiñolo A, Otero A, Prashar S. [(eta(5)-C5Me4)SiMe2(NtertBu)]TiCl2 as a pre-catalyst for the copolymerisation of ethylene with 5,7-dimethylocta-1,6-diene and with 3,7-dimethylocta-1,6-diene. Macromol Chem Phys 2002;203:139-145.

[15] Cerrada ML, Benavente R, Pérez E, Moniz-Santos J, Ribeiro MR. Metallocenic ethylene-5,7-dimethylocta-1,6-diene copolymers: structural characterization and mechanical behavior. J Polym Sci, Part B: Polym Phys 2004;42:3797-3808.

[16] Vicente AI, Campos JM, Bordado JM, Ribeiro MR. Maleic anhydride modified ethylene-diene copolymers: Synthesis and properties. React Funct Polym 2008;68:519-526.

[17] Quinn FA, Mandelkern L. Thermodynamics of crystallization in high polymers - poly-(ethylene). J Am Chem Soc 1958;80:3178-3182.

[18] Wunderlich B. Macromolecular Physics, vol. 3. New York: Academic Press; 1980. p. 42.

[19] Baltá-Calleja FJ. Microhardness relating to crystalline polymers. Adv Polym Sci 1985;66:117-148.

[20] Bunn CW. The crystal structure of long-chain normal paraffin hydrocarbons. The "shape" of the CH2 group. Trans Faraday Soc 1939;35:482-490.

[21] Shirayam K, Watabe H, Kita S. Effects of branching on some properties of ethylene alpha-olefin copolymers. Makromol Chem 1972;151:97.

[22] Popli R, Mandelkern L. The transition in ethylene co-polymers - the beta-transition. Polym Bull 1983;9:260-267.

[23] Popli R, Glotin M, Mandelkern L, Benson RS. Dynamic mechanical studies of alpha-relaxations and beta-relaxations of polyethylenes. J Polym Sci, Part B: Polym Phys 1984;22:407-448.
[24] Cerrada ML, Benavente R, Pérez E. Effect of short glass fiber on structure and mechanical behavior of an ethylene-1-octene copolymer synthesized with metallocene catalyst. Macromol Chem Phys 2001;202:2686-2695.
[25] Cerrada ML, Benavente R, Pérez E, Moniz-Santos J, Ribeiro MR. Experimental evidence of the glass transition in a metallocene ethylene-1-octene copolymer and its composites with glass fiber. Polymer 2001;42:7197-7202.
[26] Cerrada ML, Benavente R, Pérez E. Crystalline structure and viscoelastic behavior in composites of a metallocenic ethylene-1-octene copolymer and glass fiber. Macromol. Chem. Phys. 2002;203:718-726.
[27] Schatzki TF. Molecular interpretation of gamma-transition in polyethylene and related compounds. J Polym Sci, Part C-Polymer Symposium 1966;14:139.
[28] Arridge RGC. Rev Deform Behav Mater 1981;3:249.
[29] Boyd RH. Relaxation processes in crystalline polymers - molecular interpretation - a review. Polymer 1985;26:1123-1133.
[30] Benavente R, Pereña JM, Pérez E, Bello A. Relaxation processes in thermotropic polydibenzoates with oxyethylene spacers in the main-chain. Polymer 1993;34:2344-2347.
[31] Benavente R, Pereña JM, Pérez E, Bello A. Influence of annealing on the thermal and viscoelastic behavior of poly(triethylene glycol *p,p'*-dibenzoate). Polymer 1994;35:3686-3690.
[32] Heaton NJ, Benavente R, Pérez E, Bello A, Pereña JM. The gamma relaxation in polymers containing ether linkages: Conformational dynamics in the amorphous phase for a series of polybibenzoates containing oxyethylene spacers. Polymer 1996;37:3791-3798.
[33] McCrum NG, Read BE, Williams G. Anelastic and dielectric effects in polymeric solids. New York: Dover Publication, 1991.
[34] Ward IM. Mechanical Properties of Solids Polymers, 2nd. ed. Chischester: J. Wiley and Sons, 1985 (Chapter 8)